Talbot Interferometory for Imaging Two-Dimensional Electron Density Distribution over Vacuum Arc Discharge

Y. Inada[1], T. Kamiya[1], S. Matsuoka[1], A. Kumada[1], H. Ikeda[1], K. Hidaka[1]

[1] *The University of Tokyo, 3-1, Hongo, 7-chome Bunkyo-ku, Tokyo, Japan*

An electron density imaging system utilising the Talbot effect of pinhole arrays was developed for the single-shot visualisation of two-dimensional electron density distributions over pulsed millimetre-scale vacuum arc discharges. A numerical simulation using a plane wave decomposition method demonstrated the pinhole arrays with a pitch of 300μm and pinhole diameter of 150μm were most suitable for the vacuum arc measurements in the consideration of the spatial resolution and measurement accuracy. In addition, the plane wave decomposition simulation precisely expected the experimentally observed self-image behaviours of the pinhole arrays. The Talbot interferometric system was successfully used for electron density imaging over the vacuum arcs with poor reproducibility in discharge paths. The electron density images observed by the Talbot interferometer were in excellent agreement with those visualised by the previously developed Shack-Hartmann type laser wavefront sensors.

1. Introduction

We have previously reported on the development and use of highly sensitive Shack-Hartmann type laser wavefront sensors for directly imaging two-dimensional electron density distributions over extinguishing arc discharges where measurement sensitivity is improved proportionally to the focal length of microlens arrays used as the sensing element. Therefore, meniscus microlens arrays with a long focal length of ～400mm were implemented in the sensing instruments [1]. Such a long focal length was realised by the extremely sophisticated photolithography technique capable of precisely controlling the curvatures of the meniscus formation composed of the convex and concave surfaces. The optical lithography method is one of the most powerful tools for fabricating micro- and nano-structures. However, the use of the optical lithographic technology with high controllability needs a high fabrication cost, which can limit the expansion in the application range of the sensing system. Moreover, further extension of the focal lengths of microlens arrays is extremely difficult because the above-mentioned meniscus microlens arrays were fabricated with the maximum processing accuracy of the present photolithographic technique. In addition, even if an increase in the focal lengths was achieved, clear focal spot patterns could not be obtained due to the severely large diffraction limit of the microlens arrays with longer focal lengths. Therefore, in order to achieve the reduction of the fabrication cost and further improvement of the measurement sensitivity, novel electron density imaging system based on different physical phenomena should be developed without compromising an advantage of the single-shot electron density visualisation accomplished earlier [1, 2].

In this paper, we describe the feasibility study of the Talbot type laser wavefront sensors as alternative to the previously developed Shack-Hartmann type laser wavefront sensors. The Talbot interferometers install a sheet of pinhole arrays, which requires no expensive photolithographic instruments with high controllability. The sensing system has a potential of realising longer focal lengths effectively by using the Talbot effect of the pinhole arrays. A numerical simulation using a plane wave decomposition method was conducted for searching the optimal configuration of the pinhole arrays. The simulation results demonstrated that the pinhole arrays with a pitch of 300μm and pinhole diameter of 150μm were most suitable from the view points of the spatial resolution and measurement accuracy required for the electron density imaging over pulsed millimetre-scale vacuum arc discharges. The self-image behaviours of the pinhole arrays were in excellent agreement between the wavefront simulation and experimental observation. The novel system was successfully used for imaging two-dimensional electron density distributions over the vacuum arcs and it reproduced the experimental results observed by the Shack-Hartmann sensors, thus demonstrating the feasibility of using this technology.

2. Experimental details

2.1. Talbot type laser wavefront sensor

When a plane wave of a laser beam is incident upon a diffraction grating with a periodic structure, the grating image is observed repeatedly at certain lengths away from the diffraction grating [3]. This phenomenon is known as the Talbot effect, and the certain lengths and repeated grating images are called the Talbot lengths and self-images, respectively. The Talbot lengths Z_T for pinhole arrays with a lattice formation shown in Fig. 1 are given by the following equation:

$$Z_T = \frac{2d^2}{\lambda} m \quad \cdots\cdots\cdots\cdots\cdots\cdots (1)$$

where d is a pitch of pinholes, λ is the wavelength of a laser beam and m is a positive integer. In this paper, mth Talbot length means Z_T for an integer of m.

Figure 2 shows the basic concept of a Talbot type laser wavefront sensor for measuring an electron density distribution in a plasma. In the use of the pinhole arrays with the grid pattern, the self-images are composed of numerous identical optical spots arranged at the same interval. These optical spots for the Talbot sensors are shifted by the localised wavefront gradients of a laser beam, like the focal spots for the Shack-Hartmann sensors. Further, mathematical formulae demonstrate that the spot shift distance for the Talbot sensors coincides with that for the Shack-Hartmann sensors [4, 5]. Therefore, electron density measurements using the Talbot sensors can be conducted on the basis of the measurement procedure of the Shack-Hartmann sensors.

A detailed description of the experimental and analytical procedure of Shack-Hartmann sensors was previously reported [2]. The only setup difference between the Shack-Hartmann and Talbot sensors is an optical element converting laser wavefront gradients into the optical spot shifts. The conversion elements for the Shack-Hartmann sensors are microlens arrays, and those for the Talbot sensors are pinhole arrays. A Talbot sensor is composed of pinhole arrays and an image sensor. The image sensor is installed at a Talbot length and used to observe the resulting spot shifts at any given time after plasma generation. The moving distances $T(\lambda)$ for a certain wavelength λ have contribution from number densities of neutral particles, positive ions and electrons in the plasma. In particular, only the contribution from electrons depends on λ while that from neutral particles and positive ions is not influenced by λ. Therefore, our electron density measuring system employs two Talbot sensors and two lasers with different wavelengths λ_1 and λ_2 for simultaneous measurements of $T(\lambda_1)$ and $T(\lambda_2)$. The calculation of $T(\lambda_1)$-$T(\lambda_2)$ is made to eliminate the contribution from neutrals and ions and to extract electron contribution.

The Talbot sensing system described in this paper included two continuous-wave diode lasers (λ_1=784nm; λ_2=408nm) and an ICCD (intensified charge-coupled device) camera. Therefore, the temporal resolution of our Talbot sensors was determined by gating time of the ICCD camera, which was set to 2μs in this study.

2.2. Electrical circuit for arc discharge

The circuit for generating vacuum arc discharges is illustrated in Fig. 4. A 0.6μF capacitor was charged up to 32kV and through a current limiting resistance of 40Ω, positive arc discharges were generated in a 3-mm vacuum gap between rod-to-rod CuCr electrodes (Cu:Cr=75:25 wt%) of 1mm in diameter. The peak value and damping time constant of arc currents were 0.8kA and 24μs, respectively. The time when breakdown occurred was defined as t=0μs. The arc currents and arc voltages were measured by a Rogowski coil and a high voltage probe, respectively.

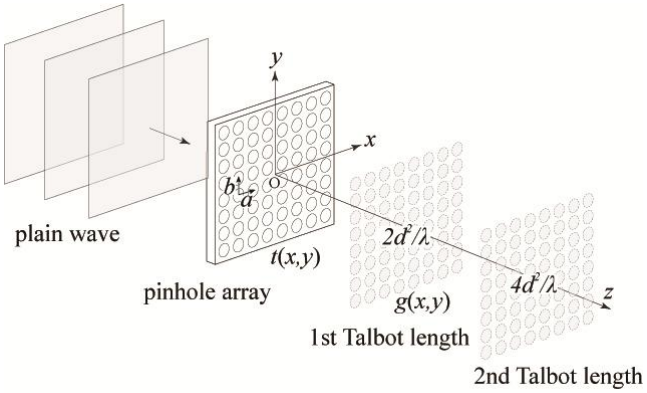

Fig.1 Talbot effect of pinhole array with lattice formation

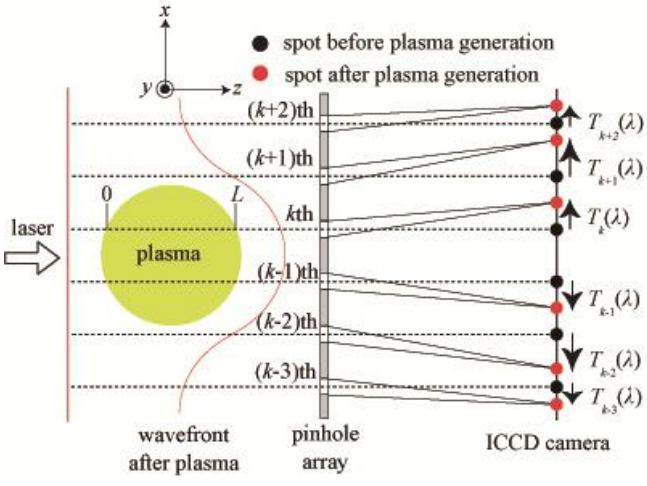

Fig.2 Talbot type laser wavefront sensor with pinhole array

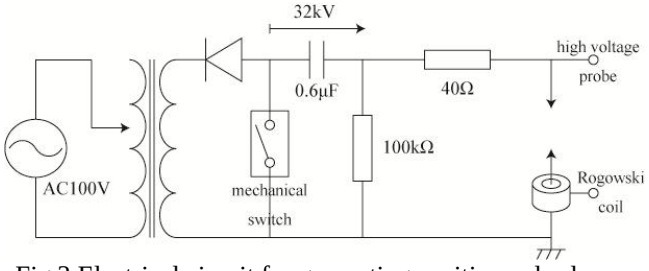

Fig.3 Electrical circuit for generating positive pulsed arc discharge in vacuum

3. Results and discussion

The optimal structure of the pinhole arrays was analytically determined by using a plane wave decomposition method. The numerical simulation was conducted for the experimental configuration in Fig. 4, where 784-nm laser beam was transmitted through a cylindrical lens with a focal length of 5m and was incident upon the pinhole arrays. In the analytical cylindrical lens test, a pitch of pinholes *d* was fixed at *d*=300μm, because *d* is equal to the spatial resolution of this Talbot system and there was a need for keeping a sufficient spatial resolution for the measurement of 3-mm vacuum arcs.

Figures 5(a)-(c) show optical spot intensity distributions for pinhole diameters *D*=100, 150 and 200μm, respectively. In the case of *D*=100μm, there were clear pseudo spots in the middle of Talbot spots. These pseudo spots prevent capturing precise focal spot positions [6] and can degrade the measurement accuracy of the Talbot sensors. The optical spot intensity distribution for *D*=200μm shows optical spots with double peaks. These double peak profiles can not represent precise focal spot positions and can also degrade the measurement accuracy. On the other hand, clear pseudo spots and double peaks were not observed in the case of *D*=150μm. Therefore, a pinhole diameter of *D*=150μm was adopted in our Talbot sensing system. Further, the validity of the simulated moving distances of optical spots *T* was experimentally confirmed by using the Talbot sensors implementing the pinhole arrays with *d*=300μm and *D*=150μm, as shown in Fig. 6.

Electron density measurements were conducted at *t*=1μs by using the Shack-Hartmann sensors and Talbot sensors. Figure 7(a) shows a two-dimensional electron density distribution over a vacuum arc discharge observed by the Shack-Hartmann sensors; Fig. 7(b), that observed by the Talbot sensors. The red and blue regions in Figs. 7(a) and (b) indicate the highest and lowest electron densities in arc channels, respectively. The order of the electron densities in these images was $10^{22}m^{-3}$, and electron densities around the anode were higher than those around the cathode. Such higher electron densities around the anode represented anode flare plasmas, which are observed in an initiation process of vacuum breakdown. Figure 7(c) shows a comparison of axial electron density distributions between the Shack-Hartmann and Talbot sensors. Considering the shot-to-shot variations in the vacuum arc discharges, the experimental result for the Talbot sensors was in excellent agreement with that for the Shack-Hartmann sensors developed earlier.

4. Conclusion

An electron density imaging system utilising the Talbot effect of pinhole arrays was developed for the single-shot visualisation of two-dimensional electron density distributions over pulsed millimetre-scale vacuum arc discharges. A plane wave decomposition simulation demonstrated the pinhole arrays with a pitch of 300μm and pinhole diameter of 150μm were most suitable for the vacuum arc measurements in the consideration of the spatial resolution and measurement accuracy. The Talbot interferometric system was successfully used for imaging electron density distributions and it reproduced the experimental results of the previously developed Shack-Hartmann sensors, thus demonstrating the feasibility of using this technology.

5. References

[1] Y. Inada, S. Matsuoka, A. Kumada, H. Ikeda, K. Hidaka, Meas. Sci. Technol. **25** (2014) 055201.

[2] Y. Inada, S. Matsuoka, A. Kumada, H. Ikeda, K. Hidaka, J. Phys. D: Appl. Phys. **45** (2012) 435202.

[3] H. F. Talbot, Philos. Mag. **9** (1836) 401.

[4] A. Momose, W. Yashiro, Y. Takeda, Y. Suzuki, T. Hattori, Jpn. J. Appl. Phys. **45** (2006) 5254.

[5] B. Platt and R. V. Schack, Opt. Sci. Cent. Newslett. **5** (1971) 15.

[6] Y. Inada, H. Matsumoto, S. Matsuoka, A. Kumada, H. Ikeda, K. Hidaka, Electr. Eng. Jpn. **181** (2012) 1.

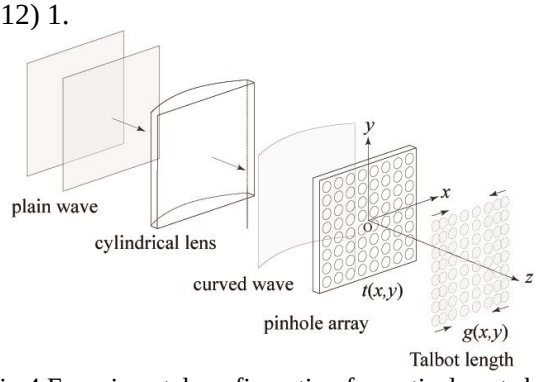

Fig.4 Experimental configuration for optical spot shift measurement

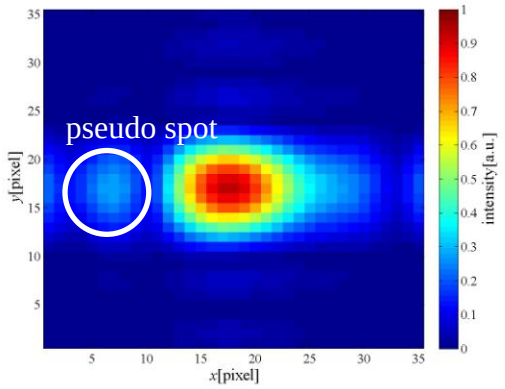

(a) D=100μm

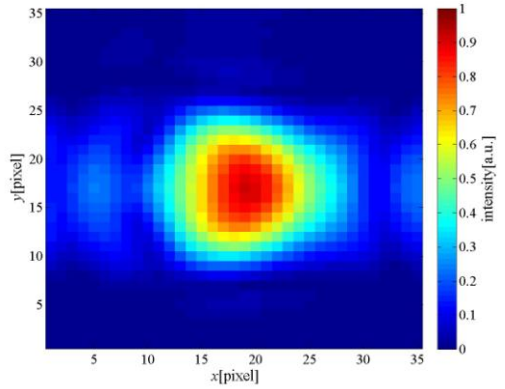

(b) D=150μm

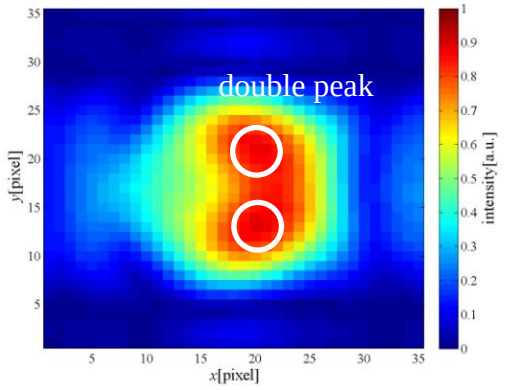

(c) D=200μm

Fig.5 Optical spot intensity distribution for 784-nm laser

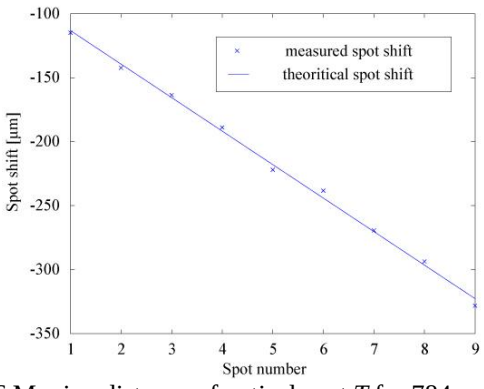

Fig.6 Moving distance of optical spot T for 784-nm laser at 2nd Talbot length

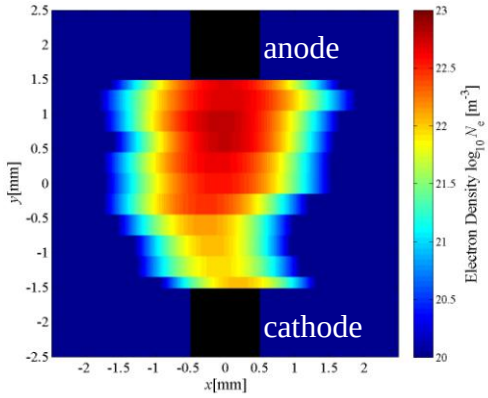

(a) Shack-Hartmann

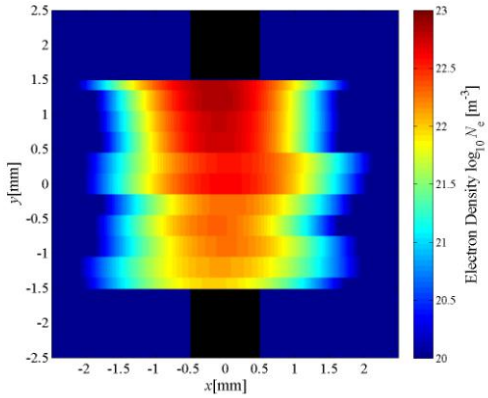

(b) Talbot

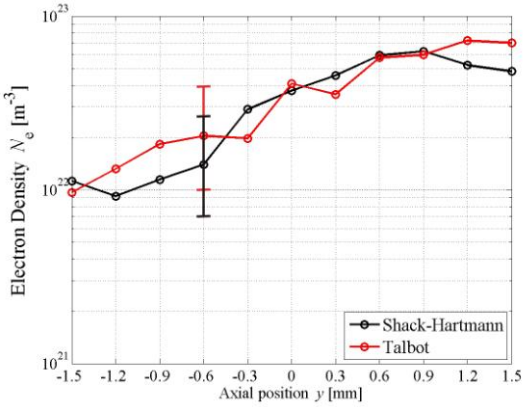

(c) comparison

Fig.7 Electron density distribution over vacuum arc discharge